Modeling Hot Wire Electrochemistry. Coupled Heat and Mass Transport at a Directly and Continuously Heated Wire

Andreas Beckmann,[†] Barry A. Coles,[‡] Richard G. Compton,[‡] Peter Gründler,*[,†] Frank Marken,[‡] and Andreas Neudeck[‡]

Universität Rostock, Abteilung für Analytische, Technische und Umweltchemie, Buchbinderstrasse 9, 18051 Rostock, Germany, and Physical and Theoretical Chemistry Laboratory, Oxford University, Oxford OX1 3QZ, U.K.

Received: August 3, 1999

Microelectrode wires heated directly in situ by an electric current generate mass as well as heat energy transport phenomena. With continuous heating, a stationary surface temperature is established as a result of thermally promoted convection. The geometry of concentration and temperature profiles under these conditions are investigated by cyclic voltammetry, potential step experiments, and finite element simulation of convection and diffusion processes. It is shown that the Nernst diffusion layer approaches a constant, temperature-independent thickness if the temperature difference between bulk and electrode surface exceeds ca. 30 K in aqueous solution. At continuously heated wire electrodes, diffusion coefficient values as well as kinetic data can be determined under well-defined temperature conditions, and in a very convenient way.

1. Introduction

Directly heated wire electrodes are not only a useful tool for analytical applications but permit analysis of the temperature dependence of electrochemical reactions. These electrochemical measurements at elevated temperatures were described elsewhere,[1−12] and the principles of this technique are explained.[6] In this method a cylindrical microelectrode is heated with a 100-kHz ac current in the heating circuit during dc polarization in the electrochemical circuit. The symmetrical electrode configuration, which allows simultaneous heating and electrochemical measurements without capacitive ac interference,[1] was achieved by using a combination of two wire electrodes with an almost identical electrical resistance (cf. Figure 1).

Two methods have been developed based on either continuous or pulsed heating. During pulsed heating the measurement takes place in the absence of convection up to 200 ms after the temperature change.[3,6,7,11] In contrast, at continuously heated electrodes convection must occur with a strong influence on the mass transport. This method is usually limited to electrode temperatures below the boiling point. Nevertheless continuous heating has the advantages of a simple measuring procedure and a constant electrode temperature during the course of the experiment. However, if pursued quantitatively, continuous heating requires that the problem of the mass transport under thermal convection and diffusion to the heated cylindrical electrodes must be solved. Fast cyclic voltammetry, short time chronoamperometry, and finite element simulation have been used for this purpose.

In a previous paper it was shown,[8] that limiting currents are obtained at a continuously heated cylindrical electrode due to thermal convection. They have been investigated and demonstrated to be scan rate independent for the same temperatures.

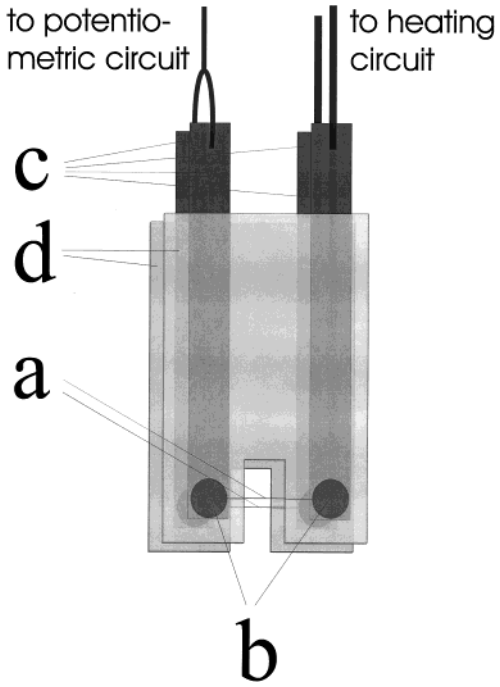

Figure 1. Scheme of the electrode construction: (a) 25 μm platinum wire (2 × 5 mm); (b) solder joints; (c) copper foils; (d) laminating foil PET/PE with adhesive E/VA.

This is in contrast to isothermal conditions where the pseudo limiting current after changing from a peak to a sigmoidal shape is never independent of the scan rate at a cylindrical electrode.[13,14] Furthermore, it was shown[8] that the temperature dependence of the limiting currents at heated wire electrodes shows an Arrhenius-type behavior as is expected based on the temperature dependence of the diffusion coefficient

$$I_{\mathrm{lim}} = I_{\mathrm{lim},\infty} e^{-E_A/RT} \qquad (1)$$

Such behavior can be explained, if the diffusion layer thickness

* Corresponding author. Phone: +49 381 498 1754. Fax: +49 381 498 1752. E-mail: peter.gruendler@chemie.uni-rostock.de.
[†] Universität Rostock.
[‡] Oxford University.

10.1021/jp992736s CCC: $19.00
Published on Web 01/12/2000

$\Delta x(T)$ in the expression which describes the limiting current under steady-state conditions

$$I_{\mathrm{lim}}(T) = \frac{zFAc_{\mathrm{bulk}}D(T)}{\Delta x(T)} \tag{2}$$

is independent of temperature. (In this equation z is the number of electrons transferred per molecule, F is Faraday's constant, A is the electrode area, c_{bulk} is the bulk concentration, Δx is the diffusion layer thickness, D is the diffusion coefficient, and I_{lim} is the limiting current at temperature T.) Paradoxically this seems to be impossible if we take into account that the velocity of the convective flow close to the electrode is increasing with the temperature. The other possibility is that $\Delta x(T)$ shows a similar temperature dependence as the diffusion coefficient, but surprisingly the determined activation energy from the temperature dependence of the limiting current is in agreement with measurements done in solvents such as acetonitrile or DMF.[15]

To resolve this apparent paradox and to develop a quantitative basis for continuously heated electrode voltammetry the mass transport conditions at a continuously heated micro wire electrode were studied by cyclic voltammetry over a wide "time window" from millivolts up to a hundred volts per second, by chronoamperometric experiments and by simulation of the limiting current employing a finite element software package. It should be noted that all experiments and the simulation refer to a horizontal electrode arrangement, as shown in Figure 1.

2. Finite Element Simulation

Simulations of the hot wire electrochemical cell were carried out using the finite element fluid dynamics program FIDAP (version 8.01)[16] on a SGI Origin 2000. For the purposes of simulation, the wire was assumed to lie horizontally in the center of a 4-mm-wide vertical channel. One-half of the vertical cross-section, i.e., from the symmetry plane to one wall, with dimensions 2 mm (horizontal) × 2.5 mm (vertical) was simulated. The wire was 0.575 mm above the lower end of the channel. The geometry and meshing were created by the GAMBIT (version 1.0) modeling and meshing program,[16] using a graded mesh with a spacing of 1 μm at the wire surface and expanding to 100 μm. The chemical system simulated contained 1 mM in aqueous solution as used for the cyclic voltammetric measurements explained in the Experimental Section.

The temperature-dependent viscosity, density, specific heat, and thermal conductivity of water were input to FIDAP as data tables using published values.[17,18] The diffusion coefficient for $[Ru(NH_3)_6]^{3+}$ determined from the fast cyclic voltammetric experiments (see below) was similarly entered as a data table, derived from

$$D_T = D_{298\mathrm{K}}e^{(E_A/R)(1/298\mathrm{K} - 1/T)} \tag{3}$$

where $D_{298\mathrm{K}} = 6.4 \times 10^{-6}$ cm^2 s^{-1} and $E_A = 13.0$ kJ mol^{-1}. Thermodiffusion was not included in the simulation, since on the assumption that the Soret coefficient $S_T < 1$,[19] the effect on the calculated limiting currents was less than 3 parts in 10^6. Boundary conditions applied were temperature (25 °C) and concentration c_{bulk} at the lower end (inlet) and at the sidewall of the channel. At the wire surface a zero concentration corresponding to the limiting current condition and a temperature T were imposed. Simulations using the successive substitution solver converged smoothly, requiring typically 2 min of CPU time. The values for the flux of chemical species to the wire, and for the heat flux, were then obtained by using functions provided in the FIDAP postprocessor.

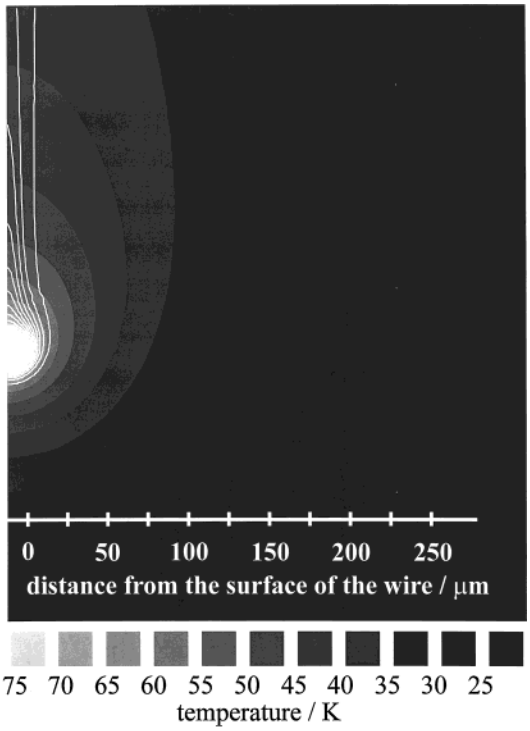

Figure 2. Temperature (interval 5 °C) and concentration (fine white contours) for a wire surface temperature of 80 °C.

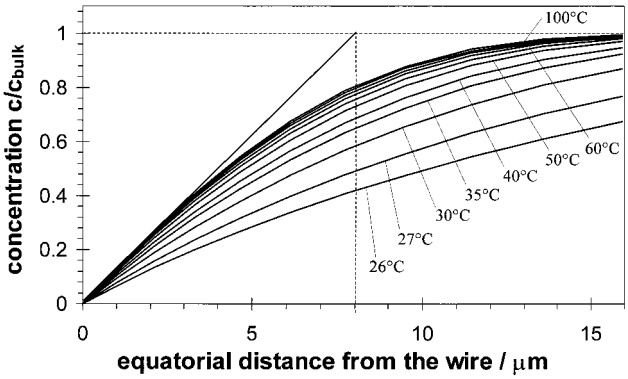

Figure 3. Concentration as a function of distance from the wire surface along a horizontal radial line, for temperatures of 26, 27, 30, 35, 40, 50, 60, 70, 80, 90, and 100 °C.

Figure 2 shows the temperature and concentration contours for a wire surface temperature of 80 °C. The gray scale indicates temperature (5 °C intervals) and shows that the thermal layer extends much further into the solution than the chemical species diffusion layer (fine white contours). Thus, most of the species diffusion is taking place within a fairly limited range of temperature on the order of 10 °C. The thickness of the species diffusion layer is fairly constant over most of the wire circumference, being slightly thinner at the lowest point on the circumference, and only increasing rapidly near the top. The concentration profile along a horizontal radial line passing through the center of the wire has been taken to be representative of the diffusion layer behavior, and these profiles are shown in Figure 3 for a range of surface temperatures from 26 to 100 °C. For temperatures of 50 °C and above, these are very similar, indicating that the diffusion layer thickness shows little further variation with temperature.

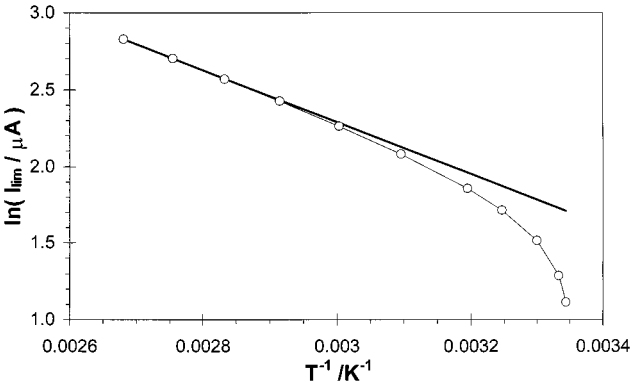

Figure 4. Arrhenius plot of the simulated limiting currents.

Figure 4 shows $\ln(I_{lim})$ plotted against *1/T* and shows that as the temperature is increased, the slope tends to a constant value. On the assumption that $I_{lim} \propto D$, this indicates a value for $E_A =$ 13.98 kJ mol^{-1}, in reasonable agreement with the value used for simulation.

3. Experimental Section

The electrode used was constructed by using a 25-μm-diameter platinum wire (99.99%, Goodfellow Cambridge, U.K.) with a total length of 7 mm (solution exposed length 5 mm) and copper foils (99.9%, Goodfellow Cambridge, U.K.) with 100-μm height and 5-mm width as contacts. The connection was obtained by using a special technique called "hot air soldering" (hot air soldering machine DRS22, ZEVAC, Switzerland) by which a very flat solder joint can be manufactured.

As isolation, laminating foils of polyester/polyethylene (PET/PE) with an adhesive ethylene vinyl acetate copolymer (E/VA) (laminating pouch film, thickness 250 μm per sheet, Ibico GmbH, Germany) as described were used.[20] The lead-in foils, the solder joint, and a part of the platinum wire (1 mm per contact side) were laminated thermally (approximately 100 °C) in such way that 5 mm of the wire can be exposed to a solution. A scheme is given in Figure 1.

Two of these electrodes were used together to obtain the symmetrical electrode assembly. In all experiments and the simulation the wire was horizontally positioned.

Temperature determination was made by using the temperature shift of the equilibrium electrode potential of a standard redox couple (temperature coefficient) equimolar in ferricyanide (99%, FISONS Loughborough Leics, U.K.) and ferrocyanide (99%, BDH Chemicals Ltd Poole, U.K.) (5 mM) with potassium chloride (99+%, Aldrich, U.K.) (0.1 M) as supporting electrolyte. The potentials were measured by means of a TEKTRONIX TDS 220 oscilloscope (supplied by S. J. Electronics, U.K.).

The cyclic voltammetric and the potential step measurements were performed on a VERSASTAT II potentiostat (EG&G Instruments Princeton Applied Research, USA).

The heating current (100 kHz ac) was generated by a function generator (Venner Electronics Ltd Surrey, U.K.) and amplifier (400-W peak power, purchased from Conrad Electronic, Germany) powered by a DC regulated power supply (13.8 V/20−22 A, Alan CTE International, Germany). The output was connected to the electrode via a transformer. The heating current was adjusted with a dual digital potentiometer (Dallas Semiconductor, USA) connected to a computer running Labview (National Instruments, USA) via a DAQ-card (AT-MIO-16XE−50, National Instruments, USA). The heating current was monitored by a TEKTRONIX TDS 220 oscilloscope (supplied by S. J. Electronics, U.K.) with a differential probe (ELDITEST, purchased from Conrad Electronic, Germany).

For the cyclic voltammetric measurements a solution of 1 mM hexaammine-ruthenium(III) chloride (98%, Aldrich, U.K.) with 0.1 M potassium chloride (99+%, Aldrich, U.K.) as supporting electrolyte in water was used. For the potential step experiments the concentration was 5 mM. All potentials were referenced to potassium chloride saturated calomel electrode (SCE) at 25 °C. A platinum plate electrode was applied as counter electrode.

All solutions were prepared by using Elgastat (High Wycombe, Bucks, U.K.) UHQ grade water with a resistivity of not less than 18 MΩ cm^{-1} and purged free of oxygen by outgassing with argon.

4. Results and Discussion

Determination of the Electrode Temperature. For the determination of the surface temperature of the heated electrode the open circuit potentiometric method was applied.[3,4,7,8,11,12] Measurements with the redox couple ferrocyanide/ferricyanide were used to relate the amplitude of the heating current to the surface temperature of the electrode. The temperature coefficient of the equilibrium potential of this redox couple (−1.6 mV K^{-1}) is applied for this purpose.[12,21,22]

Cyclic Voltammetry at Continuously Heated Cylindrical Microelectrodes. As is known from measurements using flow cells or at rotating disk electrodes it is possible to retain the peak shape behavior of cyclic voltammograms at sufficiently high scan rates even under flow conditions. This is due to the fact that the thickness of the diffusion layer under cyclic voltammetry conditions depends on the scan rate. The diffusion layer thickness at a planar electrode at the time when the peak current is observed can be simply estimated based on eq 4, which has been derived by combining the Randles Sevcik equation and eq 2 yielding Δx as a function of the scan rate v

$$\Delta x(\nu) = \frac{1}{0.44629(zF\nu/RTD)^{1/2}} \tag{4}$$

where n is the scan rate and R is the gas constant. The experimental cyclic voltammograms of 1 mM hexaammine-ruthenium(III) chloride with 0.1 M potassium chloride as supporting electrolyte in water measured at a heated cylindrical electrode (cf. Figure 5) show a peak shape at high scan rates. The change in peak current should follow the Randles Sevcik equation for a stationary planar electrode. As soon as the diffusion layer thickness reaches a critical value with decreasing scan rate, the additional mass transport caused by convection or by the influence of the cylindrical electrode geometry should cause a deviation from the predicted peak currents. Under these conditions the apparent diffusion coefficient $D_{obt,planar}(v)$, obtained from the experimental data, should increase below a critical scan rate in the $D_{obt,planar} - \log(v)$ plot. To eliminate the effect of the cylindrical diffusion the modified Randles Sevcik equation for cylindrical electrodes

$$I_{peak,cyl} = (0.44629 + 0.3435(r(zF\nu/RTD)^{1/2})^{-0.845}) \times zFAc_{bulk}D(zF\nu/RTD)^{1/2} \tag{5}$$

(derived by Neudeck and Dittrich)[23] was used. Here r is the radius of cylindrical electrode and A is the electrode area. Unfortunately, eq 5 cannot be solved algebraically to give the diffusion coefficient. However, the diffusion coefficient can be evaluated from the peak current based on eq 5 by using a simple

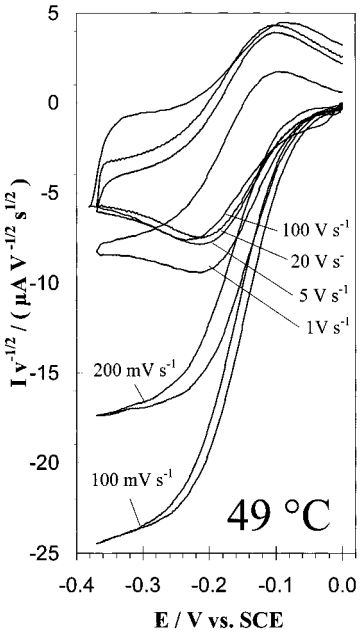

Figure 5. Cyclic voltammograms with different scan rates (100 mV s^{-1} to 100 V s^{-1}) for the reduction of 1 mM $[Ru(NH_3)_6]^{3+}$ in aqueous KCl solution at a continuously heated Pt-wire electrode ($l = 1$ cm, $d = 25$ μm) at 49 °C.

iteration procedure (e.g., *Newton's method*). The determined D_{obt} under isothermal conditions, i.e., under nonheated conditions, yields constant values as expected. At a heated electrode the D_{obt} values stay constant as well but show a sudden increase below a critical low scan rate in the $D_{obt} - \log(\nu)$ plot (cf. Figure 6). At even lower scan rates a limiting current is observed, and at higher scan rates the peak current without any influence of the thermal flux is observed.

The rate of the convective flow decreases in the direction to the electrode surface. Therefore at higher scan rates, i.e., smaller extent of the diffusion layer, less flow-dependent values for the diffusion coefficient can be measured and the real diffusion coefficient D can be expressed as the limit value of the D_{obt} values at high scan rates $D = \lim_{\nu\to\infty} D_{obt}(\nu)$. From the limiting current at scan rates below the critical scan rate and the diffusion current at high scan rates the thickness of the diffusion layer can be evaluated for each temperature at the electrode from eq 6.

$$\Delta x(T) = \frac{zFAc_{bulk}\lim_{\nu\to\infty} D_{obt}(\nu,T)}{\lim_{\nu\to 0} I_{lim}(\nu,T)} \qquad (6)$$

Surprisingly the temperature dependence of the stationary diffusion layer thickness at directly heated electrodes tends to a constant value (cf. Figure 8**)** although the flux is increased very rapidly with temperature, and due to the flux pattern the real diffusion layer thickness is not even homogeneous (cf. Figure 2).

With increasing electrode surface temperature the stationary diffusion layer thickness is decreasing very rapidly and reaches a limiting value of about 8 mm at a temperature larger than 20−30 K compared to the bulk temperature. In this region the limiting current is proportional to the real diffusion coefficient.

Chronoamperometric Experiments To Determine the Diffusion Coefficient and the Diffusion Layer Thickness at Continuously Heated Cylindrical Electrodes. The same information about the thickness of the diffusion layer at continuously heated

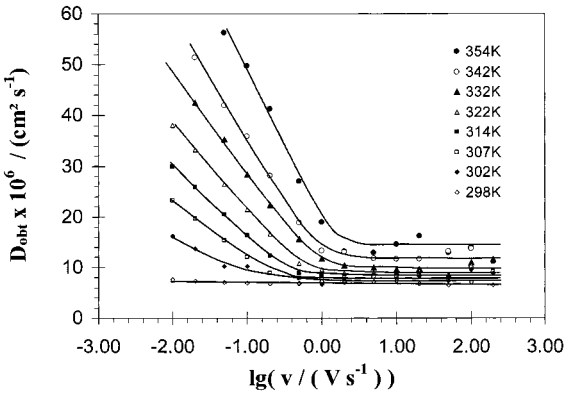

Figure 6. Obtained diffusion coefficients from the peak or steady-state currents of cyclic voltammograms with different scan rates (10 mV s^{-1} to 200 V s^{-1}) of 1 mM $[Ru(NH_3)_6]^{3+}$ in aqueous KCl solution (0.1 M) at a continuously heated Pt wire electrode ($l = 1$ cm, $d = 25$ μm) at different temperatures (25−81 °C).

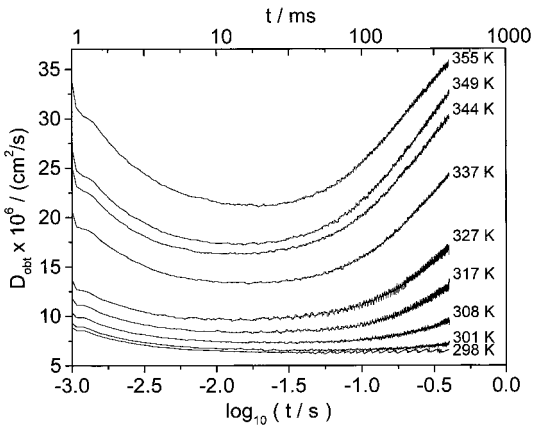

Figure 7. Plot of the obtained diffusion coefficients D_{obt} from chronoamperometric experiments (by use of the modified Cottrell equation for cylindrical electrodes) at a continuously heated Pt-wire electrode ($l = 1$ cm, $d = 25$ μm) of 5 mM $[Ru(NH_3)_6]^{3+}$ in an aqueous KCl solution (0.1 M) for different temperatures (25−82 °C).

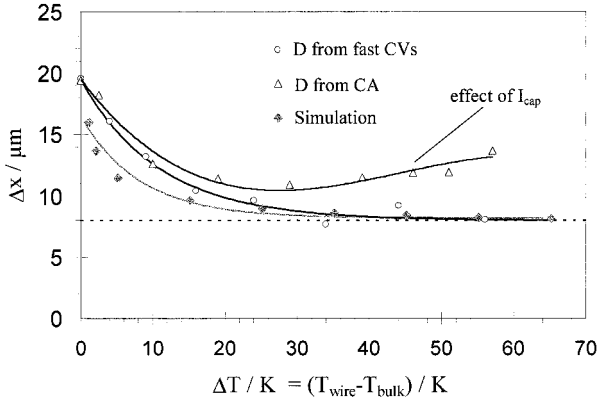

Figure 8. $\Delta x(T)$ calculated from experimental and simulated limiting currents I_{lim} and from the determined diffusion coefficients by fast cyclic voltammetry, short time chronoamperometry, and using $D(25\ °C) = 6.1 \times 10^{-6}$ cm^2 s^{-1} and $E_A = 14.6$ kJ mol^{-1} (0.151 eV) in case of the simulation, respectively.

cylindrical electrodes are available by so-called Cottrell experiments.[24] After a period of time in the range of several milliseconds necessary to charge the electrochemical double layer the current at the continuously heated wire electrodes follows the Cottrell equation. For longer time scales the current does not follow the Cottrell equation due to the influence of

the cylindrical diffusion (dependent on the radius of the electrode and the diffusion constant) together with that of thermal convection.

As in the case of the Randles Sevcik equation the appropriately corrected Cottrell equation has been already derived for cylindrical electrodes[25]

$$I(t) = \frac{zFADc_{\text{bulk}}}{r} f_{\text{cyl}}\left(\frac{Dt}{r^2}\right) \tag{7}$$

where the f_{cyl} with $\chi = Dt/r^2$ can be approximated as

$$f_{\text{cyl}}(\chi) = \frac{e^{-0.1(\pi\chi)1/2}}{(\pi\chi)^{1/2}} + \frac{1}{\ln(5.2945 + 1.4986(\chi^{1/2}))} \tag{8}$$

where z is the number of electrons transferred per molecule, F is Faraday's constant, A is the electrode area, D is the diffusion coefficient, c_{bulk} is the bulk concentration, and r is the radius of the cylindrical electrode.

As in the case of the modified Randles Sevcik equation the D_{obt} values can be calculated by an iteration procedure at each time of the chronoamperometric experiment. The plot of the obtained diffusion coefficients based on the cylindrical Cottrell equation versus the logarithm of the time (cf. Figure 7) shows a similar behavior as the D_{obt} values from cyclic voltammograms (the slow scan rates correspond to the long times in the Cottrell experiments).

At long time scales the apparent D_{obt} values show a sudden increase due to the increase of the influence of the thermal convection on the expanding diffusion layer similar to the influence on the peak current at slowly recorded cyclic voltammograms. At very short times $t < 10$ ms the D_{obt} values are also increasing. This is due to the fact that the Faradaic current is superimposed on a capacitive current. The resulting current is larger and yields an increase in the D_{obt} value calculated on the basis of the Cottrell equation. Because of this barrier to the low time scale it is more difficult to obtain the true diffusion coefficient from the limit value of the obtained D_{obt} value $D = \lim_{t\to 0} D_{\text{obt}}(t)$. However, the $D_{\text{obt}} - \log t$ plots at temperatures less than 337 K show a plateau (cf. Figure 7**)** which permits the estimation of the real D value from this wide-range minimum. At higher temperatures the approximation yields large diffusion coefficients due to interference of the higher and slower decreasing capacitive currents and the earlier starting and stronger influence of the convection. Therefore these values are marked as capacitive effect in Figures 8 and 9. Nevertheless, the values were used to calculate the stationary diffusion layer thickness by using eq 2 and the corresponding limiting current obtained at the end of the chronoamperometric experiments. The obtained temperature dependence of the stationary diffusion layer thickness $\Delta x(T)$ is in good agreement with the $\Delta x(T)$ values derived from the cyclic voltammograms but shows an increase at high temperatures due to the capacitive effect described above (cf. Figure 8).

The temperature dependence $Dx(T)$ obtained from the limiting current of cyclic voltammograms at low scan rates and the calculated D values from the peak currents at high scan rates are in better agreement with the simulations than the data from chronoamperometric experiments. This is due to the fact that the influence of the capacitive current was diminished by background correction of the cyclic voltammograms, which was not applicable to the chronoamperometric data due to the signal shape during the first milliseconds. The $\Delta x(T)$ plot derived from the cyclic voltammetry as well as from the simulation ($D_{298\text{K}} = 6.4 \times 10^{-6}$ cm^2 s^{-1}, $E_A = 13$ kJ mol^{-1}) surprisingly shows that the stationary diffusion layer thickness tends to a constant value with increasing surface temperature of the electrode, although the thermal flux is strongly increased.

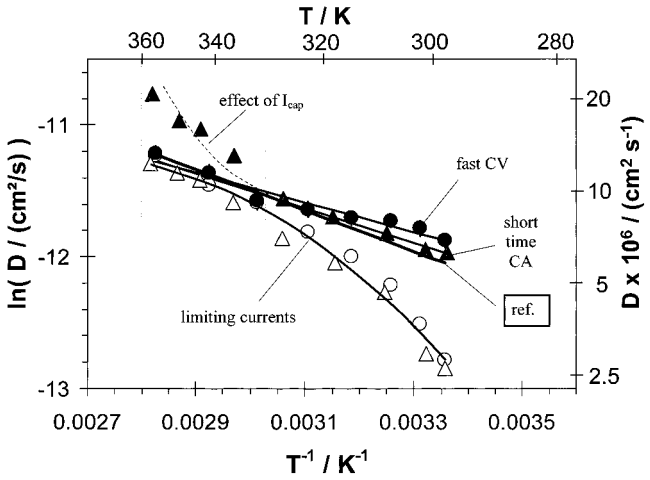

Figure 9. Arrhenius plots of the limiting currents and the determined diffusion coefficients from fast cyclic voltammetry and short time chronoamperometry at a continuously heated cylindrical micro wire electrode including a reference plot for $E_A = 13$ kJ mol^{-1}.[26]

The Arrhenius plots of the D values from the chronoamperometric and cyclic voltammetric measurements were used to determine the activation energy of the diffusion (cf. Figure 9). The plot of the $D(T)$ values derived from the peak currents of cyclic voltammograms at high scan rates is in agreement with the reference measurement calculated from limiting currents at a micro disk electrode in a thermostated cell but with a higher standard deviation. The chronoamperometrically determined D values show a much smaller standard deviation and a good agreement at low temperatures but due to the "capacitive effect" discussed above the values tend to differ at temperatures higher than 30 K above the starting temperature. For high temperatures the limiting currents of cyclic voltammograms at low scan rates as well as the steady-state currents determined from chronoamperometric measurements show the smallest standard deviation. Therefore these limiting currents are suitable for the measurement of the activation energy of the diffusion constant as well as other temperature-dependent parameters of more complex reaction mechanisms.

As it can be seen from eq 2 the $D(T)$ dependence can be derived from the limiting currents at a heated cylindrical electrode when the temperature dependence $Dx(T)$ is known. This dependence derived from cyclovoltammetric and chronoamperometric experiments as well as from finite element simulation clearly shows that the limiting diffusion layer thickness defined by eq 2 (cf. Figure 8), which represents an average diffusion layer thickness at a heated cylindrical electrode, tends to a constant value with increasing temperature very rapidly. At a temperature difference between the electrode and the solution of 30 K the deviation is less than 10% from the high-temperature limit. This permits the determination of the activation energy of the diffusion coefficient by eq 1 in this temperature range just from the $\ln(I_{\text{lim}})$ versus T^{-1} plot. For this purposes it is not necessary to know Dx. However, Figure 9 shows additionally the $D(T)$ values calculated from the limiting currents by use of $Dx = 8$ mm as it was found for temperatures larger than 30 K beyond the temperature of the bulk solution. The data are in good agreement with the reference data in this temperature range.

5. Conclusions

The problem of coupled heat and mass transport processes at a continuously heated micro wire electrode in aqueous solution can be characterized by the following peculiarities.

(1) The temperature profile expands into solution much further than any concentration profile that could be generated by electrochemical processes. Temperature differences inside any diffusion layer are low. Consequently, electrochemical reactions including transport processes proceed under nearly uniform temperature conditions. At continuously heated electrodes, real values for the diffusion coefficient at electrode surface temperature can be determined.

(2) The Nernst diffusion layer approaches a constant thickness if the temperature difference between bulk and electrode surface exceeds ca. 30 K. As a result, diffusion-limited current values of cyclic voltammetry and chronoamperometry can be evaluated directly.

(3) The geometry of both temperature and concentration profiles is well defined and reproducible. Under conditions of continuous heating, kinetic data can be determined in a simple way.

(4) In nonaqueous solvents, a modified value of the constant Nernst layer can be expected to be valid due to differences in viscosity, thermal conductivity, etc. Nevertheless, fundamental results hold true also if the solvent is changed. The measuring technique can be extended to such systems.

Acknowledgment. Andreas Beckmann thanks St. John's College, Oxford, for financial support. Frank Marken thanks the Royal Society for the award of a University Research Fellowship and New College, Oxford, for a Stipendiary Lectureship. Financial support of the Deutsche Forschungsgemeinschaft is gratefully acknowledged.

References and Notes

(1) Gründler, P.; Tadesse Zerihun; Kirbs, A.; Grabow, H. *Anal. Chim. Acta* **1995**, *305*, 232.

(2) Gründler, P.; Kirbs, A. Patent DE 195 43 060.3, **1995**.

(3) Gründler, P.; Kirbs, A. *Analyst* **1996**, *121*, 1805.

(4) Tadesse Zerihun; Gründler, P. *J. Electroanal. Chem.* **1996**, *404*, 243.

(5) Tadesse Zerihun; Gründler, P. *J. Electroanal. Chem.* **1996**, *415*, 85.

(6) Gründler, P. *Fresenius J. Anal. Chem.* **1998**, *362*, 180.

(7) Kirbs, A. Dissertation Universität Rostock, 1999.

(8) Beckmann, A.; Schneider, A.; Gründler, P. *Electrochem. Commun.* **1999**, *1*, 46.

(9) Jasinski, M.; Kirbs, A.; Schmehl, M.; Gründler, P. *Electrochem. Commun.* **1999**, *1*, 26.

(10) Voss, T.; Gründler, P.; Brett, C. M. A.; Oliveira Brett, A. M. *J. Pharm. Biomed. Anal*. **1999**, *19*, 127.

(11) Gründler, P.; Kirbs A. *Electroanalysis* **1999**, *11* (4), 223.

(12) Tadesse Zerihun Dissertation Universität Rostock, 1997.

(13) Aoki, K.; Honda, K.; Tokunda, K.; Matsuda, H. *J. Electroanal. Chem.* **1985**, *182*, 267.

(14) Kovach, P. M.; Caudrill, W. L.; Peters, D. G.; Wightman, R. M. *J. Electroanal. Chem.* **1985**, *185*, 285.

(15) Jacob, S. R.; Qi Hong; Coles, B. A.; Compton, R. G. *J. Phys. Chem. B* **1999**, *103*, 2963.

(16) Fluent Europe Ltd., Sheffield, U.K.

(17) Weast, R. C. *Handbook of Chemistry and Physics*, 55th ed.; CRC Press: Cleveland, OH, 1974.

(18) Lide, D. R. *Handbook of Chemistry and Physics*, 74th ed.; CRC Press: Boca Raton, FL, 1993.

(19) Kondepudi, D.; Prigogine, I. *Modern Thermodynamics*; Wiley: New York, 1998.

(20) Neudeck, A.; Kress, L. *J. Electroanal. Chem.* **1997**, *437*, 141.

(21) Bard, A.J.; Parsons, R.; Jordan, J. *Standard Potentials in aqueous solutions*; Marcel Dekker: New York, 1985.

(22) Compton, R. G.; Coles, B. A.; Marken F. *Chem. Commun.* **1998**, 2595.

(23) Neudeck, A.; Dittrich, J. *J. Electroanal. Chem.* **1991**, *313*, 37.

(24) Cottrell, F. G. *Z. Pysik. Chem.* **1902**, *42*, 385.

(25) Amatore, C. Electrochemistry at Ultramicroelectrodes. In *Physical Electrochemistry—Principles, Methods, and Applications*; Rubinstein, I., Ed.; Marcel Dekker: New York, 1995.

(26) Compton, R. G.; Marken, F.; Roberts, S. L. To be submitted for publication.